



Grain structure effect on quench sensitivity of Al–Zn–Mg–Cu–Cr alloy

Cheng-bo LI^{1,2,3}, Su-qi HAN^{1,2,4}, Sheng-dan LIU^{1,2,4}, Yun-lai DENG^{1,2,4}, Xin-ming ZHANG^{1,2,4}

1. School of Materials Science and Engineering, Central South University, Changsha 410083, China;

2. Key Laboratory of Nonferrous Metal Materials Science and Engineering, Ministry of Education, Central South University, Changsha 410083, China;

3. Light Alloy Research Institute, Central South University, Changsha 410083, China;

4. Nonferrous Metal Oriented Advanced Structural Materials and

Manufacturing Cooperative Innovation Center, Central South University, Changsha 410083, China

Received 30 September 2015; accepted 27 April 2016

Abstract: The effect of grain structure on quench sensitivity of an Al–Zn–Mg–Cu–Cr alloy was investigated by hardness testing, optical microscopy, X-ray diffraction, scanning electron microscopy, transmission electron microscopy and scanning transmission electron microscopy. The results show that with the decrease of quenching rate from 960 °C/s to 2 °C/s, the hardness after aging is decreased by about 33% for the homogenized and solution heat treated alloy (H-alloy) with large equiaxed grains and about 43% for the extruded and solution heat treated alloy (E-alloy) with elongated grains and subgrains. Cr-containing dispersoids make contribution to about 33% decrement in hardness of the H-alloy due to slow quenching; while in the E-alloy, the amount of (sub) grain boundaries is increased by about one order of magnitude, which leads to a further 10% decrement in hardness due to slow quenching and therefore higher quench sensitivity.

Key words: grain structure; Al–Zn–Mg–Cu–Cr alloy; dispersoids; quench sensitivity

1 Introduction

Al–Zn–Mg–Cu alloys are often quench sensitive, i.e., their hardening capability by aging decreases after slow quenching from solution heat treatment temperature. Quench sensitivity receives great influence from chemical compositions, such as main alloying elements Zn, Mg, Cu [1–4], and trace elements like Cr, Mn, Zr and Sc [5–7]. The addition of trace elements gives rise to the formation of fine dispersoids, which can inhibit recrystallization and grain growth and therefore improve properties remarkably [8–12]. However, the presence of these dispersoids may increase quench sensitivity because coarse quench-induced particles often form on them preferentially during slow quenching [2,3,13]. As a result, fewer η' hardening precipitates can be obtained after subsequent aging, which leads to lower hardness and strength. Al_3Zr dispersoids are often small and coherent with Al matrix, and therefore lead to low quench sensitivity; however, they may lose coherency

with Al matrix due to recrystallization and become preferential nucleation sites for quench-induced phase, and consequently increase quench sensitivity [14,15]. By contrast, Cr-containing dispersoids often lead to very high quench sensitivity [3,7], because they are large and incoherent with Al matrix and act as effective heterogeneous nucleation sites.

Apart from dispersoids, grain structure can have great influence on quench sensitivity. Subgrain boundaries and especially grain boundaries have high interfacial energy, and thus there is a strong tendency for heterogeneous precipitation to occur at them during slow quenching [6,13]; consequently, quench sensitivity is increased [16,17]. An increased number and misorientation angle of subgrain boundaries can give rise to higher quench sensitivity of Al–Zn–Mg–Cu alloys such as 7055 and 7050 aluminum alloys [17,18]. The degree of recrystallization has effect on quench sensitivity. For instance, DORWARD and BEERNTSEN [19] reported that with recrystallization fraction increasing from 15% to 80% in 7050 aluminum alloy, the strength reduction

due to slow quenching increased from 6% to 12%. However, the effect of grain structure on quench sensitivity relative to hardness and strength was not fully understood because of the complex microstructure due to partial recrystallization in these alloys. In the Zr-containing alloys, the occurrence of recrystallization changes the number of (sub)grain boundaries and characteristics of Al_3Zr dispersoids as well. During slow quenching, heterogeneous precipitation can form both at (sub)grain boundaries and on Zr-containing dispersoids located in the recrystallized and unrecrystallized regions [17,18]. Therefore, it is difficult to distinguish their respective contribution to quench sensitivity.

In this work, an attempt has been made to further understand grain structure effect on quench sensitivity by using a fully homogenized ingot and an extruded rod of Al–Zn–Mg–Cu–Cr 7075 aluminum alloy. The ingot and rod have the same chemical compositions but very different grain structure. It is well known that the interface between Cr-containing dispersoids and Al matrix is unlikely to change much after recrystallization [7], so it is probably to distinguish the contribution of Cr-containing dispersoids from that of grain structure to quench sensitivity.

2 Experimental

The studied materials were cut from a fully homogenized ingot and an extruded rod of high strength aluminum alloy with the chemical composition of Al–5.74Zn–2.74Mg–1.75Cu–0.27Cr–0.15Fe–0.086Si (mass fraction, %). After solution heat treatment at 470 °C for 1 h, the specimens were subjected to end quenching test, room temperature (RT) water quenching and boiling water quenching to obtain different quenching rates. Thermocouples were inserted into the specimens to record time–temperature data to estimate quenching rate. End quenching test led to quenching rates from 2 °C/s to 11 °C/s through the critical temperature range of 415–185 °C; while RT water and boiling water quenching led to a high quenching rate of about 960 °C/s and 100 °C/s, respectively. After quenching, the specimens were aged at 120 °C for 24 h in an air furnace. For convenience, the homogenized and solution heat treated alloy was named H-alloy, and the extruded and solution heat treated alloy was named E-alloy.

The Vickers hardness testing was performed on the aged specimens with a load of 3 kg, and five measurements were made to obtain an average value. Specimens for grain structure examination were ground, polished and etched by Graff Sargent's reagent (1 mL HF, 16 mL HNO_3 , 3 g CrO_3 and 83 mL distilled water), and then observed by a MX3000 microscope. Second phase

in the as-quenched specimens was examined by X-ray diffraction (XRD) performed on a Rigaku D/Max 2500 diffractometer. Some aged specimens were examined using FEI Quanta–200 scanning electron microscopy (SEM), JEM–2100F transmission electron microscopy (TEM) and Tecnai G² F20 S-Twin scanning transmission electron microscopy (STEM). Specimens for SEM examination were ground and polished. Specimens for TEM and STEM examination were thinned to about 0.08 mm, electro-chemically polished using solution of 20% HNO_3 + 80% CH_3OH below –20 °C.

3 Results

3.1 Hardness curves

The hardness of the aged specimens is plotted as a function of quenching rate in Fig. 1(a). The shape of hardness curves is quite different for the H-alloy and the E-alloy. For the H-alloy, the hardness does not change above about 10 °C/s, but drops rapidly at lower quenching rate; while for the E-alloy, the hardness decreases slightly in the range of 1000–100 °C/s and then more rapidly with a further decrease of quenching rate. Above about 100 °C/s, the E-alloy exhibits slightly

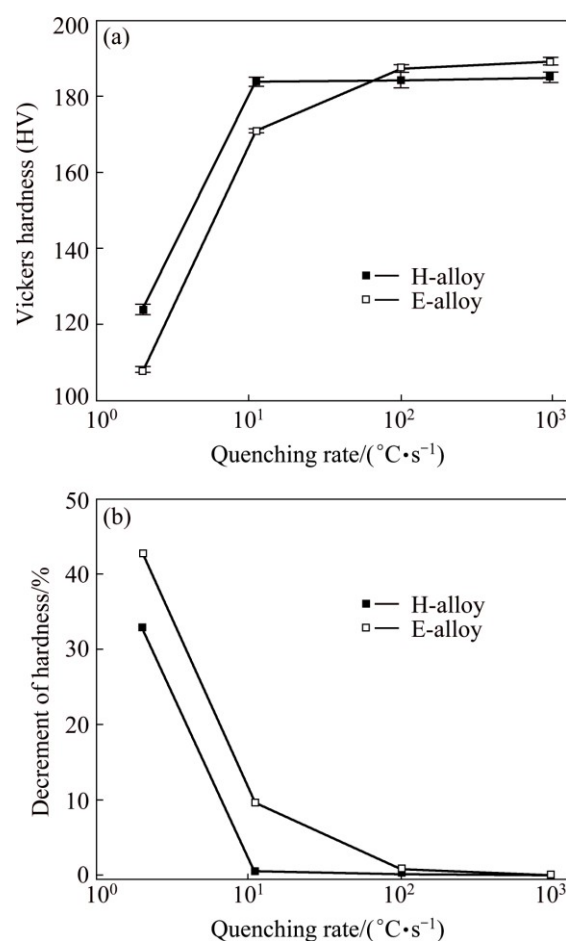


Fig. 1 Effect of quenching rate on hardness (a) and decrement of hardness (b) of aged specimens

higher hardness than the H-alloy; at lower quenching rates, the H-alloy exhibits higher hardness.

The decrement of hardness, D_H , due to slow quenching can be used to evaluate quench sensitivity. It is calculated by

$$D_H = (H(960) - H(X)) / H(960) \times 100\% \quad (1)$$

where $H(960)$ and $H(X)$ denote the hardness of the specimens quenched at 960 °C/s and X °C/s, respectively. A larger value of D_H means higher quench sensitivity. Based on the data in Fig. 1(a), the values of D_H were calculated and given in Fig. 1(b). It can be seen that the E-alloy shows higher quench sensitivity than the H-alloy; at the quenching rate of 2 °C/s, the decrement of hardness is approximately 43% for the E-alloy and 33% for the H-alloy.

3.2 Microstructure

Figure 2 shows typical optical micrographs of the

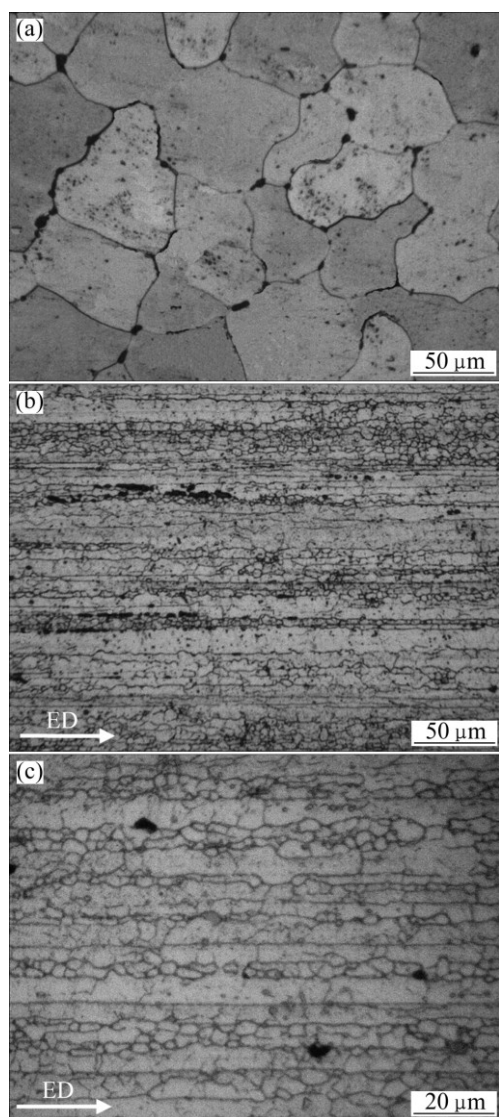


Fig. 2 Optical micrographs of H-alloy (a) and E-alloy (b, c) (ED: Extrusion direction)

studied alloys after solution heat treatment. It can be seen that there is a large difference in the grain structure. In the H-alloy, there are large equiaxed grains with a size (equivalent circle diameter) about 90 μm, as shown in Fig. 2(a). In the E-alloy, however, the grains are elongated along the extrusion direction (Fig. 2(b)), and there are a number of well defined subgrains with an average size of about 3.7 μm (Fig. 2(c)). The length of grain boundaries in the H-alloy was estimated to be about 0.029 m/mm², while in the E-alloy, the length of grain boundaries and subgrain boundaries was about 0.251 m/mm².

It is known that quench sensitivity relative to hardness is primarily dependent on the amount of quench-induced phase, which decreases the solutes available for hardening precipitates during subsequent aging; consequently, hardness and strength are decreased [13,17]. XRD, SEM, TEM and STEM were used to examine these microstructural features in both H-alloy and E-alloy, and some typical results are given in Figs. 3–8.

Figure 3 shows XRD traces of the specimens of H-alloy and E-alloy after quenching. In the specimens cooled at 960 °C/s, it seems that only the peaks of Al solid solution can be identified for both alloys. While in the specimens cooled at 2 °C/s, apart from peaks of Al solid solution, peaks of η (MgZn₂) phase and T (Al₂Mg₃Zn₃) phase may be identified. Therefore, it is reasonable to conclude that slow quenching led to the formation of η and T phases in both H-2 and E-2 specimens. However, the diffraction intensity of η phase seems to be obviously larger for the E-2 specimen than the H-2 specimen, which may indicate a larger amount of η phase in the former specimen. The diffraction intensity of T phase is similar for both specimens, which may indicate a similar amount of T phase in them.

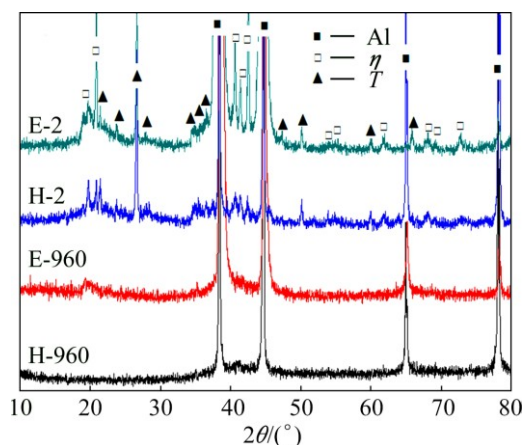


Fig. 3 XRD traces of as-quenched specimens (H-960 and H-2 mean the specimen of H-alloy cooled at 960 °C/s and 2 °C/s, respectively; E-960 and E-2 mean the specimen of E-alloy cooled at 960 °C/s and 2 °C/s, respectively)

Figure 4 shows typical SEM images of the aged H-alloy and E-alloy cooled at 2 °C/s. As expected, quench-induced phase can be detected in the interior of grains and at (sub)grain boundaries. In the interior of grains, most quench-induced phase particles were associated with Cr-containing dispersoids. Figure 5 gives a high angle annular dark field (HAADF) image of the

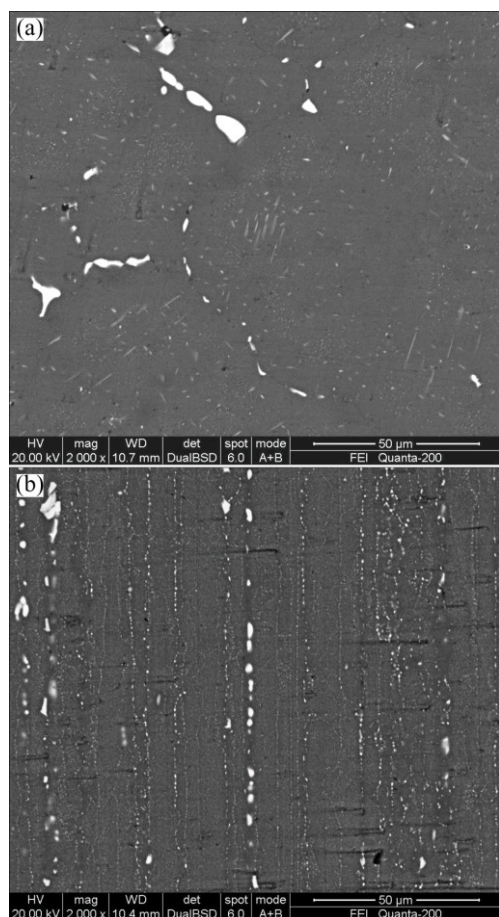


Fig. 4 Typical SEM images of aged H-alloy (a) and aged E-alloy (b) cooled at 2 °C/s

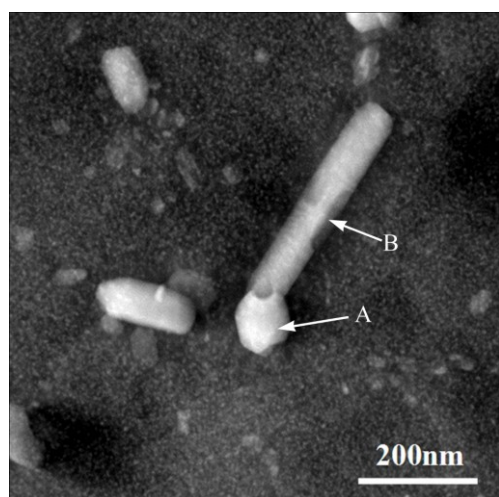


Fig. 5 HAADF image showing quench-induced particle nucleated on Cr-containing dispersoids in aged E-alloy cooled at 2 °C/s (A–Cr-containing dispersoids; B– η phase)

aged E-alloy cooled at 2 °C/s. EDS examination showed that particle A contains 13.36% Zn, 8.72% Mg, 4.16% Cu, 3.77% Cr and 69.99% Al (mass fraction); therefore, it is likely the Cr-containing dispersoids and their size is about 80 nm. These dispersoids are generally incoherent with the Al matrix and act as preferential nucleation sites for heterogeneous precipitation during slow quenching [3,7]. As a result, a large quench-induced particle B with a length about 400 nm can be observed to associate with particle A; EDS examination showed that this particle contains 19.69% Zn, 13.13% Mg, 12.39% Cu and 54.79% Al (mass fraction), and it is likely the η phase.

TEM examination showed that quench-induced particles were made up of η phase and T phase in the interior of grains, which is the same as the results shown in Fig. 3. As an example, Fig. 6 shows TEM bright field image and $\langle 111 \rangle_{\text{Al}}$ selected area diffraction pattern (SADP) of the aged H-alloy cooled at 2 °C/s. According to the morphology and SADP, the lath-like particles are likely η phase, while those plate-like ones are likely T phase. They have been observed in previous investigations [20,21]. Due to their anodic nature, some quench-induced η phase particles were etched out during specimen preparation, leaving white holes; while few T phase particles were etched out, which is likely because they are more resistant to corrosion. The quench-induced particles were quite large and unlikely to have hardening effect; simultaneously they consumed a number of Zn and Mg solutes in the solid solution, and consequently fewer hardening precipitates were obtained after subsequent aging. Around these particles, there were soft zones free of hardening precipitates, as shown in Fig. 6.

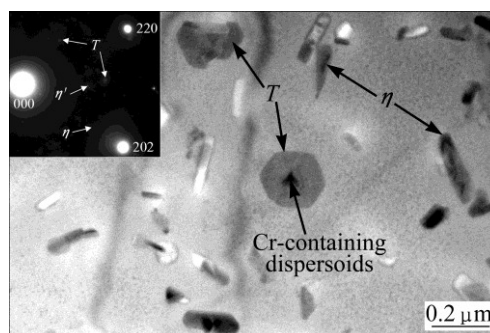


Fig. 6 TEM bright field image and $\langle 111 \rangle_{\text{Al}}$ selected area diffraction pattern of aged H-alloy cooled at 2 °C/s

Grain boundaries and subgrain boundaries, due to their high interfacial energy, often act as preferential nucleation sites for quench-induced precipitation during slow quenching [13,17,22,23]. As a result, most grain boundaries and subgrain boundaries were covered by quench-induced particles in the slowly-quenched specimens (Fig. 4); therefore, the shape of grains and

subgrains was revealed. Slow quenching gives rise to loss of solutes and vacancies near grain and subgrain boundaries, and consequently there were precipitate free zones (PFZ) adjacent to them after subsequent aging, as shown in Fig. 7. The PFZ exhibits white contrast due to lack of hardening precipitates, while the matrix far from the grain boundaries is covered by a number of precipitates and therefore exhibits gray contrast.

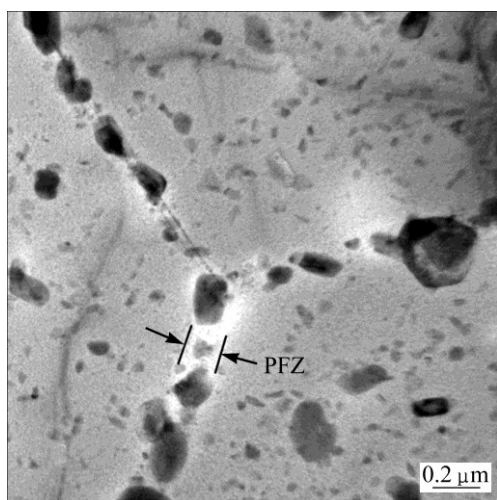


Fig. 7 TEM bright field image of aged specimen of E-alloy cooled at 2 °C/s

From Fig. 4, it seems that there is a larger amount of quench-induced particles in the E-alloy than H-alloy after slow quenching. Based on five images, the area fraction of these particles was estimated to be about 7.0% in the E-alloy cooled at 2 °C/s, but about 3.6% in the H-alloy cooled at 2 °C/s. Combined with the results in Fig. 3, the 3.4% increment of the amount of quench-induced particles in the E-alloy was probably attributed to η phase formed at (sub)grain boundaries during slow quenching. Therefore, the presence of (sub)grain boundaries did not change the type of quench-induced phase but increased their amount significantly. Moreover, it can be seen from Fig. 4 that apart from quench-induced particles there are some larger white particles with a size of about several microns. EDS analysis showed that they were S (Al_2CuMg) phase and Fe-containing phase, which often exist in 7xxx series alloys [17,21]. In the H-alloy, these particles were primarily located at grain boundaries; in the E-alloy, these particles were crashed and distributed along the extrusion direction. According to a previous investigation [17], these particles may have minor effect on quench sensitivity.

4 Discussion

The H-alloy and E-alloy have the same chemical compositions, but E-alloy exhibits higher quench

sensitivity relative to hardness. This is likely due to the fact that there is a larger amount of quench-induced particles in the E-alloy subjected to slow quenching. According to microstructural examination, it is because the amount of nucleation sites for heterogeneous precipitation is different in the studied alloys. In the H-alloy, Cr-containing dispersoids and grain boundaries can act as nucleation sites for heterogeneous precipitation; while in the E-alloy, Cr-containing dispersoids, grain boundaries and subgrain boundaries are such nucleation sites. Now it is required to distinguish their respective contribution to quench sensitivity.

It was shown that for the homogenized and solution heat treated 7055 Al alloys with and without Zr, the drop percentage in hardness was lower than about 2% with quenching rate decreasing from 170 °C/s to 2 °C/s [17]. In these alloys, the grain size was about 42 and 50 μm , respectively; so the contribution of grain boundaries to quench sensitivity was quite small, about 2%. In the H-alloy, the grains were larger with a size of about 90 μm , which resulted in fewer grain boundaries; therefore, it is reasonable to believe that the contribution of grain boundaries to quench sensitivity was minor. The 33% drop in hardness with quenching rate decreasing from 960 °C/s to 2 °C/s was primarily the contribution of Cr-containing dispersoids in this alloy.

Cr-containing dispersoids are incoherent with the Al matrix [3,7], and it is believed that the number and feature of Cr-containing dispersoids were similar in the H-alloy and E-alloy. Therefore, the contribution of dispersoids to quench sensitivity was the same for both alloys. However, the drop percentage in hardness of the E-alloy was increased to 43% with quenching rate decreasing from 960 °C/s to 2 °C/s. Compared with the H-alloy, the amount of subgrain and grain boundaries was increased by about one order of magnitude in the E-alloy, which resulted in a larger amount of quench-induced phase in this alloy cooled at 2 °C/s (Fig. 4). In the zones near subgrain and grain boundaries, there were few hardening precipitates; consequently, these zones are soft. A larger amount of subgrain and grain boundaries led to a higher volume of soft zones, i.e., fewer hardening precipitates were obtained in the matrix. This definitely gave rise to lower hardness of this specimen after aging. Therefore, in the E-alloy, subgrain and grain boundaries made contribution to about 10% drop in hardness due to slow quenching and increased quench sensitivity.

5 Conclusions

1) With the decrease of quenching rate from 960 °C/s to 2 °C/s, the decrement of hardness was 33%

and 43%, respectively, for the H-alloy and E-alloy.

2) In both alloys, η and T phases form during slow quenching; grain structure changes the amount rather than the type of quench-induced phase.

3) In the H-alloy, Cr-containing dispersoids are the main heterogeneous nucleation sites and have significant effect on quench sensitivity, and they result in about 33% drop in hardness due to slow quenching; while grain boundaries make a minor contribution to quench sensitivity.

4) In the E-alloy, Cr-containing dispersoids, subgrain and grain boundaries are preferential nucleation sites for quench-induced precipitation; the amount of subgrain and grain boundaries is increased by one order of magnitude, and consequently the quantity of quench-induced particles are increased significantly, which leads to a further 10% drop in hardness due to slow quenching and therefore higher quench sensitivity.

References

- [1] LIU S, ZHONG Q, ZHANG Y, LIU W, ZHANG X, DENG Y. Investigation of quench sensitivity of high strength Al–Zn–Mg–Cu alloys by time-temperature-properties diagrams [J]. *Materials and Design*, 2010, 31: 3116–3120.
- [2] DENG Y, WAN L, ZHANG Y, ZHANG X. Influence of Mg content on quench sensitivity of Al–Zn–Mg–Cu aluminum alloys [J]. *Journal of Alloys and Compounds*, 2011, 509: 4636–4642.
- [3] LIM S T, YUN S J, NAM S W. Improved quench sensitivity in modified aluminum alloy 7175 for thick forging applications [J]. *Materials Science and Engineering A*, 2004, 371: 82–90.
- [4] GARCIA-CORDOVILL A C, LOUIS E. A differential scanning calorimetry investigation of the effects of zinc and copper on solid state reactions in Al–Zn–Mg–Cu alloys [J]. *Materials Science and Engineering A*, 1991, 132: 135–141.
- [5] QI X H, DENG Y L, LIU S D, ZHANG Y Y, ZHANG X M. Effect of minor Sc on quench sensitivity of 7085 aluminum alloy [J]. *The Chinese Journal of Nonferrous Metals*, 2013, 23: 666–672. (in Chinese)
- [6] LIU Sheng-dan, ZHANG Xin-ming, CHEN Ming-an, YOU Jiang-hai, ZHANG Xiao-yan. Effect of Zr content on quench sensitivity of AlZnMgCu alloys [J]. *Transactions of Nonferrous Metals Society of China*, 2007, 17: 787–792.
- [7] SHARMA M M. Microstructural and mechanical characterization of various modified 7XXX series spray formed alloys [J]. *Materials Characterization*, 2008, 59: 91–99.
- [8] FANG H C, CHEN K H, CHEN X, HUANG L P, PENG G S, HUANG B Y. Effect of Zr, Cr and Pr additions on microstructures and properties of ultra-high strength Al–Zn–Mg–Cu alloys [J]. *Materials Science and Engineering A*, 2011, 528: 7606–7615.
- [9] FANG H C, CHAO H, CHEN K H. Effect of Zr, Er and Cr additions on microstructures and properties of Al–Zn–Mg–Cu alloys [J]. *Materials Science and Engineering A*, 2014, 610: 10–16.
- [10] SENATOROVA O G, UKSUSNIKOV A N, LEGOSHINA S F, FRIDLINDER I N, ZHEGINA I P. Influence of different minor additions on structure and properties of high-strength Al–Zn–Mg–Cu alloy sheets [J]. *Materials Science Forum*, 2000, 331–337: 1249–1254.
- [11] MILMAN Y V, SIRKO A I, LOTSKO D V, SENKOV O, MIRACLE D B. Microstructure and mechanical properties of cast and wrought Al–Zn–Mg–Cu alloys modified with Zr and Sc [J]. *Materials Science Forum*, 2002, 396: 1217–1222.
- [12] ZOU Liang, PAN Qing-lin, HE Yun-bin, WANG Chang-zhen, LIANG Wen-jie. Effect of minor Sc and Zr addition on microstructures and mechanical properties of Al–Zn–Mg–Cu alloys [J]. *Transactions of Nonferrous Metals Society of China*, 2007, 17: 340–345.
- [13] LI Pei-yue, XIONG Bai-qing, ZHANG Yong-an, LI Zhi-hui, ZHU Bao-hong, WANG Feng, LIU Hong-wei. Quench sensitivity and microstructure character of high strength AA7050 [J]. *Transactions of Nonferrous Metals Society of China*, 2012, 22: 268–274.
- [14] SCHÖBEL M, PONGRATZ P, DEGISCHER H P. Coherency loss of Al₃(Sc, Zr) precipitates by deformation of an Al–Zn–Mg alloy [J]. *Acta Materialia*, 2012, 60: 4247–4254.
- [15] KANNO M, OU Bin-lung. Heterogeneous precipitation of intermediate phases on Al₃Zr particles in Al–Cu–Zr and Al–Li–Cu–Zr alloys [J]. *Materials Transactions*, 1991, 32: 445–450.
- [16] LIU S D, LI C B, DENG Y L, ZHANG X M. Influence of grain structure on quench sensitivity relative to localized corrosion of high strength aluminum alloy [J]. *Materials Chemistry and Physics*, 2015, 167: 320–329.
- [17] LIU S, LIU W, ZHANG Y, ZHANG X, DENG Y. Effect of microstructure on the quench sensitivity of AlZnMgCu alloys [J]. *Journal of Alloys and Compounds*, 2010, 507: 53–61.
- [18] ZHANG X M, LIU W J, LIU S D, ZHOU M Z. Effect of processing parameters on quench sensitivity of an AA7050 sheet [J]. *Materials Science and Engineering A*, 2011, 528: 795–802.
- [19] DORWARD R C, BEERNTSEN D J. Grain structure and quench-rate effects on strength and toughness of AA7050 Al–Zn–Mg–Cu–Zr alloy plate [J]. *Metallurgical and Materials Transactions A*, 1995, 26: 2481–2484.
- [20] TANG Jian-guo, CHEN Hui, ZHANG Xin-ming, LIU Sheng-dan, LIU Wen-jun, OUYANG Hui, LI Hong-ping. Influence of quench-induced precipitation on aging behavior of Al–Zn–Mg–Cu alloy [J]. *Transactions of Nonferrous Metals Society of China*, 2012, 22: 1255–1263.
- [21] YANG X B. Research on microstructure and properties of Al–Zn–Mg–(Cu) alloy after different heat treatment [D]. Changsha: Hunan University, 2014. (in Chinese)
- [22] LIU S, LI C, HAN S, DENG Y, ZHANG X. Effect of natural aging on quench-induced inhomogeneity of microstructure and hardness in high strength 7055 aluminum alloy [J]. *Journal of Alloys and Compounds*, 2015, 625: 34–43.
- [23] LIU S D, CHEN B, LI C B, DAI Y, DENG Y L, ZHANG X M. Mechanism of low exfoliation corrosion resistance due to slow quenching in high strength aluminium alloy [J]. *Corrosion Science*, 2015, 91: 203–212.

晶粒组织对 Al-Zn-Mg-Cu-Cr 合金 淬火敏感性的影响

李承波^{1,2,3}, 韩素琦^{1,2,4}, 刘胜胆^{1,2,4}, 邓运来^{1,2,4}, 张新明^{1,2,4}

1. 中南大学 材料科学与工程学院, 长沙 410083;
2. 中南大学 有色金属材料科学与工程教育部重点实验室, 长沙 410083;
3. 中南大学 轻合金研究院, 长沙 410083;
4. 中南大学 先进有色金属结构材料与制造协同创新中心, 长沙 410083

摘要: 采用硬度测试、光学显微镜、X-射线衍射、扫描电镜、透射电镜和扫描透射电镜等手段研究了晶粒组织对 Al-Zn-Mg-Cu-Cr 合金淬火敏感性的影响。结果表明: 淬火速率从 960 °C/s 减小至 2 °C/s 时, 均匀化及固溶后合金(H-合金)时效后的硬度下降了约 33%, 而挤压及固溶后合金(E-合金)时效后的硬度下降了约 43%。H-合金中有粗大等轴状晶粒, E-合金中有拉长的变形晶粒及亚晶粒。慢速淬火 H-合金硬度下降 33%是由含 Cr 弥散粒子引起的; E-合金中(亚)晶界的数量增加了大约一个数量级, 导致慢速淬火试样硬度的下降幅度进一步增加了 10%, 淬火敏感性更高。

关键词: 晶粒组织; Al-Zn-Mg-Cu-Cr 合金; 弥散粒子; 淬火敏感性

(Edited by Yun-bin HE)